# A Novel Nonaxisymmetric Endwall Contouring for Turbine Cascade Using Automated Optimization

Desheng Chen[1], Bo Liu[2], Lei Wang[3], Zhenzhe Na[4], Zhiyuan Cao[5], Jian Huang[6]

Northwestern Polytechnical University, Xi'an, China

[1]chendesheng152@126.com; [2]liubo704@nwpu.edu.cn; [3]recoba201@gmail.com;

[4]na_wuli@163.com; [5]zylast@126.com; [6]huangjian051634@126.com

***Abstract*-A novel nonaxisymmetric endwall contouring is presented to suppress corner separation and produce more uniform exit flow angle. Firstly, a design methodology of automated optimization based on a baseline cascade is put forward. Then with respect to the contoured endwall and the baseline cascade, numerical simulation is conducted in an effort to further the understanding of the effects of endwall contouring. The results demonstrate that with nonaxisymmetric endwall, the corner separation is enormously suppressed owing to the redistribution of the blade loading in the blade passage. Furthermore, the total loss coefficient is decreased by 10% in the 128%$C_{ax}$plane, and the flow turning angle becomes larger, which clarifies the mechanisms of reduction in secondary flow losses.**

***Keywords-Secondary Flow Loss; Nonaxisymmetric Endwall Contouring; Corner Separation***

## I. INTRODUCTION

Nowadays, the improvement of turbine efficiency has a large influence on the overall gas turbine performance. Various researches are available in the literature to minimize the overall losses, and thus improve turbine efficiency. Moreover, endwall losses play a significant role in the overall losses. Hence it becomes necessary to learn about the mechanisms of secondary loss as well as to establish the design methods to reduce the losses. Most previous optimization efforts concentrate mostly on altering rotor and stator blade shapes. However, the application of nonaxisymmetric endwall to minimize secondary flow losses in the blade passage is still considered a hot field of research.

Dejc [1] was the first to put forward the concept of contouring endwall shape, and many later investigations were based on his proposed geometries. Morris and Hoare [2] performed experiments according to Dejc's geometries, and the experiment results showed a reduction of total pressure loss close to the nonaxisymmetric endwall of 25% for a low aspect ratio airfoil. Then, for reducing the secondary flow loss, Rose [3] initially proposed nonaxisymmetric endwall contouring, which was focused on equalizing the endwall pressure field. Hartland et al. [4] and Gregory-Smith et al. [5] performed experiments in the Durham cascade with two nonaxisymmetric endwalls, and the results showed considerable loss reduction. Based on the previous work from the Durham cascade investigation, Brennan et al. [6] and Rose et al. [7] redesigned the endwalls in a high pressure (HP) turbine, whose results demonstrated that the turbine efficiency increases by about 0.6%.

This paper presents the development of a novel non-axisymmetric endwall design in a turbine cascade, which is focused on the suppression of corner separation. Figure 1 visualizes the streamlines on the suction surface of a blade from the baseline cascade, and a corner vortex can be easily detected, which contributes significantly to the secondary losses in the blade passage.

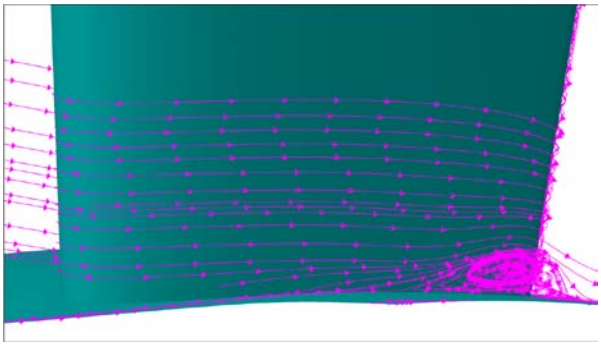

Fig. 1 Streamlines around the suction surface of a blade, basline cascade

## II. DESIGN PROCEDURES

### A. Baseline Geometry

The design procedures are carried out on a high pressure turbine vane cascade with moderate blade loading. Table Ⅰ provides a brief overview of the flow and geometric parameters of the investigated baseline cascade.

TABLE Ⅰ FLOW AND GEOMETRIC PARAMETERS OF BASELINE CASCADE

| Parameters | Units | Values |
|---|---|---|
| No. of Blades | 1 | 33 |
| Blade Axial Cord | mm | 30.45 |
| Pitch | mm | 57.12 |
| Blade Span | mm | 40 |
| Hub Radius | mm | 300 |
| Blade Aspect Ratio | 1 | 0.665 |
| Inlet Flow Angle | deg | 0 |
| Exit Flow Angle | deg | 79.5 |

### B. Endwall Design Principles

In the open literature, there are mainly two kinds of mechanisms accounting for the secondary flow loss reduction with nonaxisymmetric endwall configuration [8]. One mechanism attributes the secondary flow losses to the cross-passage pressure gradient, whereas the other mechanism considers the way in which the horse vortex forms to be the key factor that affects the generation of secondary flows. Through further investigation, the blade loading redistribution in the blade passage may be also responsible for the reduction of secondary flow losses. On the one hand, the transverse pressure gradient has a large impact on the blade loading distribution; on the other hand, the blade loading distribution has much to do with the way in which the horse vortex forms.

Hence, the combination of the three previously mentioned factors may pave the way for further investigations on the mechanisms of the generation of secondary flows and the approaches to minimize the resulting losses.

### C. Endwall Design Methodology

#### 1) Endwall Parametrization:

An area which ranges from the leading edge to the trailing edge is selected, which is limited by the suction surface and the pressure surface of an adjacent blade in the circumferential direction. In an effort to parameterize the area, several cuts are carried out along a virtual streamline. The streamline is aligned with the blade camber curve. The blade passage is divided into five cuts, each with a distance of 25% of the blade channel width to the adjacent one. Seven parameters are chosen along each cut homogeneously. Thus, twenty-eight free control points are available for the automated optimization.

#### 2) Endwall Optimization:

The optimization system of NUMECA/Design3D is used to conduct the optimization process. In this process, the radial coordinates of the previously mentioned twenty-eight control points are selected as the free parameters. The objective function is to minimize the total pressure loss while maintaining the mass flow rate constant. With respect to the algorithms, a neural network is used to predict the aerodynamic performance of endwall contours that are not part of the already generated database, whereas a genetic algorithm is applied to search for a better design while carrying out the optimization process. Figure 2 presents the generated height contour of the optimal contoured endwall in the blade-to-blade passage, which ranges from the entry to the exit in the axial direction.

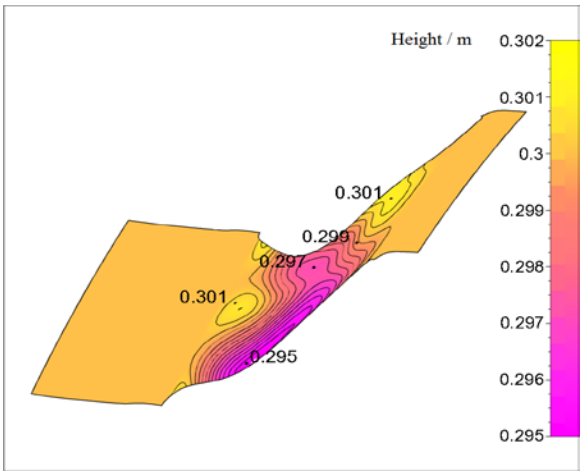


Fig. 2 Height contour (contoured endwall)

## III. NUMERICAL APPROACH

In an effort to analyze the detailed flow phenomena in the endwall region, steady numerical simulation with a 3D-RANS flow solver including an S-A turbulence model is carried out through the system of NUMECA/Fine turbo. The global mean residue is required to be less than 1×10exp(-6). A fine multi-block grid of nearly 0.6 million nodes with an O4H topology is applied for sufficiently resolving the blade boundary layer and the endwall boundary layer. Total pressure, total temperature, and axial flow direction are needed as the inlet boundary conditions, and static pressure is selected as the outlet boundary condition.

## IV. RESULTS AND DISCUSSION

### A. Loss Characteristics

The application of nonaxisymmetric endwall contouring leads to a modified loss characteristics for the turbine cascade. Figure 3a displays the numerical results for the spanwise total pressure loss coefficient distributions (pitchwise-averaged) at 128%Cax, which covers half a blade span.

The total pressure loss coefficient is defined by

$$C_p^* = \frac{P_{t,1} - P_{t,2}}{P_{t,1}} \quad (1)$$

The figure clarifies that the contoured endwall creates a redistribution in the losses near endwall region, whereas the losses between z/h=0.36 and 0.5 remain unchanged. In detail, the losses are decreased to a large extent between z/h=0.04 and 0.18, while a slight loss increase can be detected between z/h=0.2 and 0.36 as well as between the endwall and z/h=0.04. Hence, the total pressure loss (mass averaged) is decreased by 10% in this plane.

Figures 3b and 3c separately present the numerical results of the total pressure loss with respect to the baseline cascade and the contoured endwall at 128% Cax, which is shown in arrange, covering one pitch and half a blade span.

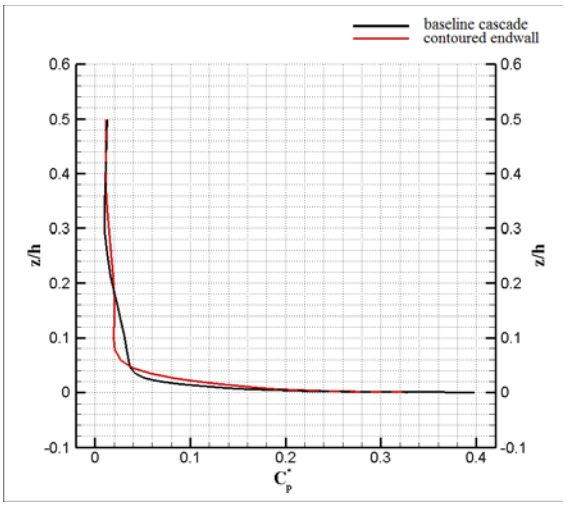


Fig. 3a Pitch averaged total pressure loss coefficient distributions at 128% Cax

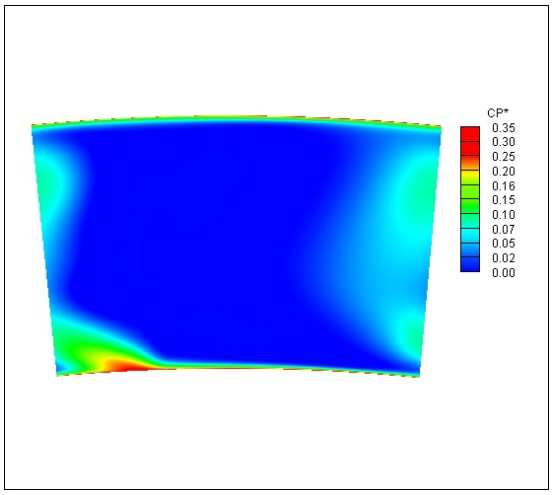


Fig. 3b Total pressure loss contour at 128% Cax, baseline cascade

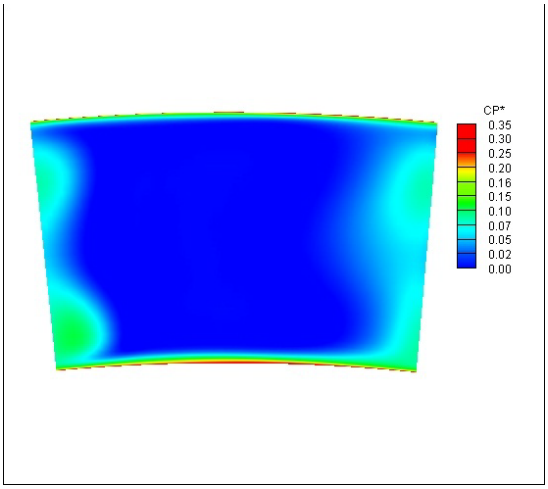


Fig. 3c Total pressure loss contour at 128% Cax, contoured endwall

For the baseline cascade, an area with high losses resulting from the corner separation can be easily detected, whereas for the contoured endwall, the scale of the high loss area is much smaller, which can be attributed to the suppression of hub-corner separation. Additionally, comparing the contoured endwall with the baseline cascade, the loss intensity is reduced, and the maximum loss is reduced from 0.3 to 0.2 according to the numerical results.

### *B. Exit Flow Angles*

The spanwise distributions of the exit flow angles for the baseline and the contoured endwall are shown in Figure 4 at 128% Cax. As can be seen in this figure, a significant modification of the exit flow angle distribution (pitch averaged) can be detectable at 128% Cax, for the application of non-axisymmetric endwall reduces the underturning of the flows to a large degree. In detail, the underturning, which is mainly caused by the blockage of the previously mentioned corner separation, is decreased by 9.5°in the near endwall region, whereas it is increased by 1°at 30% blade span, which overall leads to a reduction in the underturning of the flows in the blade passage. Hence a more homogeneous and balanced spanwise distribution of the flow turning can be achieved with the contoured endwall.

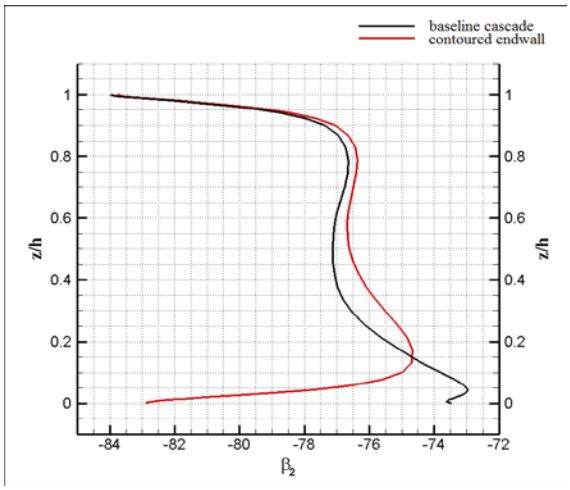


Fig. 4 Outflow angle distributions at 128% Cax

### *C. Blade Surface Pressure Distributions*

The blade surface static pressure distributions, namely blade loading distributions, near the endwall are manifested in Figure 5a from the leading edge to the trailing edge in the axial direction for the baseline cascade and the contoured endwall. In this figure, a redistribution of the blade loading from the leading edge to the trailing edge can be visible with the contoured endwall. Furthermore, comparing the contoured endwall with the baseline cascade, the blade loading is decreased between Cax=20% and 65%. In this case, the circumferential pressure gradient, also known as driving force of the secondary flows, is considerably reduced and thus the resulting secondary flow loss is remarkably reduced; whereas the blade loading is increased between Cax=0% and 20% as well as between Cax=65% and 80%. Hence in these two ranges the driving force of the secondary flows is increased owing to the increased circumferential pressure gradient. However, it still has a good impact on the flows in the blade passage, which will be discussed in the following subsection. In summary, the modified blade loading distribution exerts a positive effect on the development of vortex structures in the blade passage, which is closely linked with the secondary flows in the blade passage.

Figures 5b and 5c present the static pressure contour together with streamlines near the endwall region for the baseline cascade and the contoured endwall, respectively.

Comparing Figures 5b and 5c, the extent of hub-corner separation can be easily detected. Moreover, regarding the contoured endwall, between Cax =0% and 20%, the static pressure gradient is almost perpendicular to the streamlines. As is mentioned above, the blade loading in this range is increased, so the driving force is beneficial to the flows in the blade passage. Concerning the contoured endwall, between Cax=65% and 80%, the static pressure gradient is almost parallel to the streamlines. Thus, the previously mentioned higher blade loading in the circumferential direction enhances the cross flows from the pressure side to the suction side, which causes the loss core to migrate from the hub endwall to the suction surface, and the migration of low momentum fluid is responsible for the reducing or avoiding the hub-corner separation. By nature, with the addition of the contoured endwall, the modified blade loading distribution changes the flow structures in the blade passage, which contributes to the suppression of hub-corner separation and the resulting reduction in secondary flow losses.

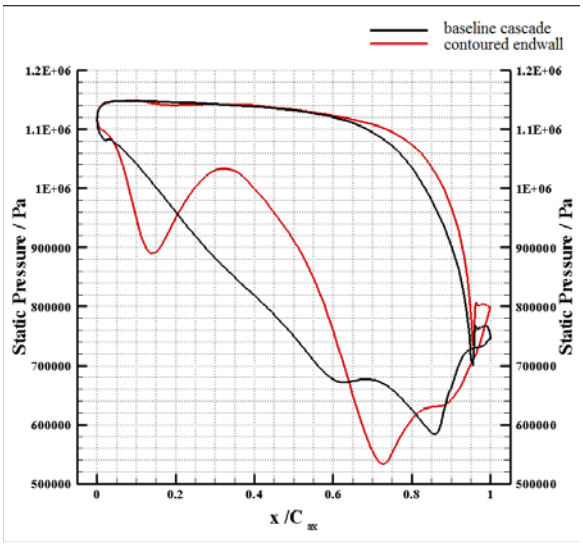


Fig.5a Blade static pressure distributions

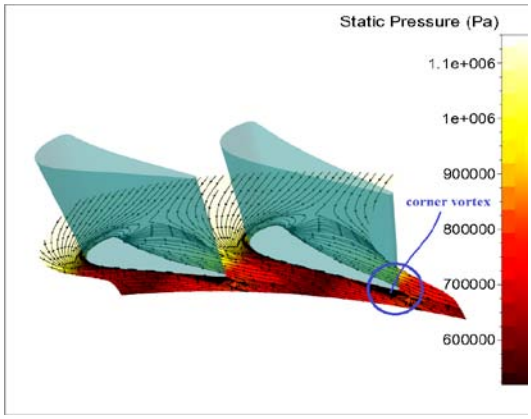


Fig.5b Static pressure contour with streamlines near the endwall, baseline cascade

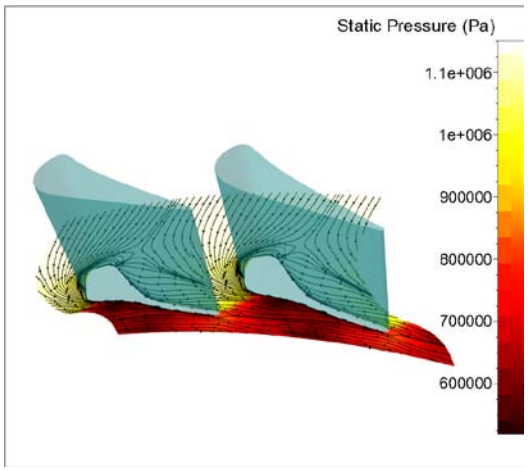


Fig.5c Static pressure contour with streamlines near the endwall, contoured endwall

### *D. Corner Separation*

The corner separation is clearly shown in Figures 6a and 6b where the detail of the flows around the trailing edge and the suction surface is separately visualized for the baseline cascade. In these figures, the green colored lines clusters represent the streamlines around the endwall, the light blue colored lines clusters represent the streamlines around the suction surface, and the pink colored lines clusters represent the streamlines in the blade passage, especially near the rear part of the blade passage. As is mentioned above, a considerable hub-corner separation can be easily detected, which can be attributed to the interaction between the passage vortex and the boundary layers of both the suction surface and the hub endwall. Then huge secondary flow losses are caused by the severe hub-corner separation, which can be clarified by the underturning of the passage flows shown in Figure 4.

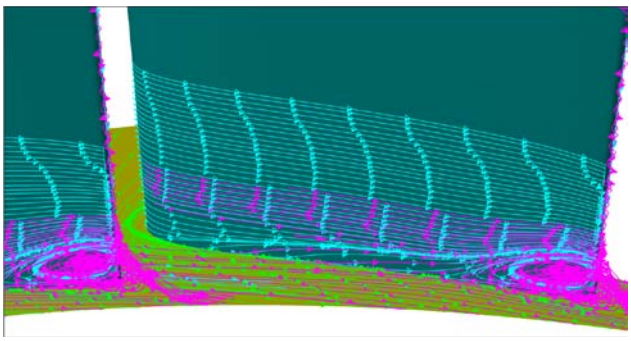

Fig. 6a Streamlines around trailing edge, baseline cascade

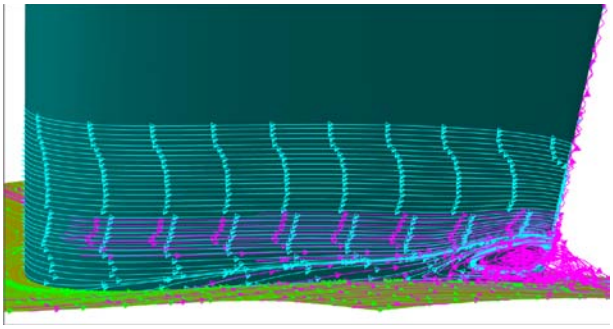

Fig.6b Streamlines around suction surface, baseline cascade

Figures 7a and 7b separately visualize the detail of the flows around the trailing edge and the suction surface for the contoured endwall. The three kinds of colored lines clusters share the identical meaning with the lines clusters shown in Figures 6a and 6b. Comparing Figure 7a and 6a, the hub-corner separation is suppressed to a huge extent, which acts as the key factor in reducing the secondary flow losses in the blade passage. As is previously mentioned, the higher driving force in the circumferential direction caused by the increased blade loading near the trailing edge makes the passage vortex core to migrate from the hub-endwall to the suction surface. Through this process the low momentum fluid is almost moved away from the original high loss region, which results in the suppression of the hub-corner separation and the reduction in secondary flow losses.

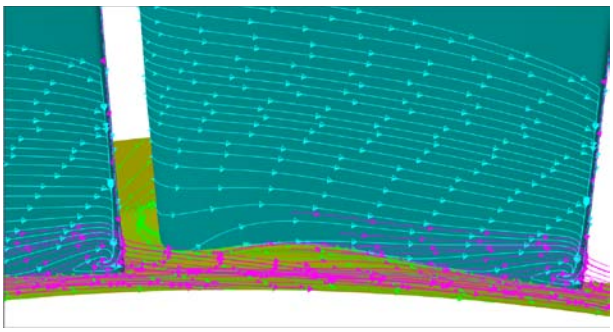

Fig. 7a Streamlines around trailing edge, contoured endwall

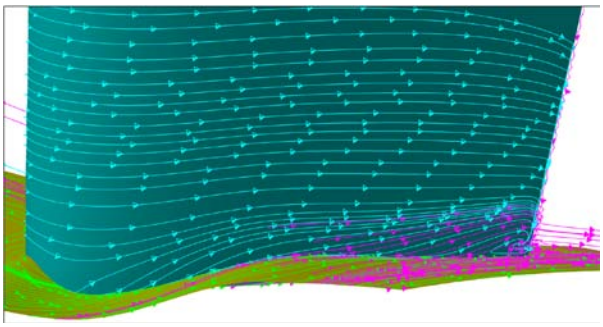

Fig. 7b Streamlines around suction surface,contoured endwall

## V. CONCLUSION AND OUTLOOK

A novel nonaxisymmetric endwall has been numerically designed and investigated in detail in this paper. Concerning the contoured endwall, the hub-corner separation is enormously suppressed and the interaction between the low momentum endwall fluid and the suction surface boundary layer is greatly decreased, which can be attributed to the modified flow structures in the blade passage. Hence, the total pressure loss coefficient is decreased by 10% in the 128%$C_{ax}$ plane.

In the future, common design rules should be developed in order to further the understanding of the mechanisms of secondary flows in the blade passage. Moreover, concerning compressors, nonaxisymmetric endwall contouring will still be a field of research.

In summary, nonaxisymmetric endwall contouring has been a powerful tool to minimize secondary flow losses, and it has the potential for further improving the efficiency of modern turbomachinery and gas turbines.

## NOMENCLATURE

| | |
|---|---|
| $\beta$ | Flow Angle |
| $C_{ax}$ | Axial Cord Length |
| $C_p^*$ | Total Pressure Loss Coefficient |
| P | Static Pressure |
| h | Blade Span |
| z | Span Direction Coordinate |

## SUBSCRIPTS

| | |
|---|---|
| 1 | Inlet Plane |
| 2 | Outlet Plane |
| t | Total |

## ACKNOWLEDGMENT

This paper is supported by the National Natural Science Foundation of China (50976093). Furthermore, the authors appreciate Xiaoyue Zhang for her editorial assistance.

## REFERENCES

[1] Dejc, M.E. et al., 1960, "Method of Increasing the Efficiency of Turbine Stages with Short Blades", Teploenergetica, No. 2, Translation No. 2816, Associated Electrical Industries Ltd.

[2] Morris, A.W.H., Hoare, R.G., 1975, "Secondary Loss Measurements in a Cascade of Turbine Blades with Meridional Wall Profiling", ASME Paper 75-WA/GT-13

[3] Rose, M. G., 1994, "Non-Axisymmetric Endwall Profiling in the HP NGV's of an Axial Flow Gas Turbine," ASME Paper No. 249-GT-94.

[4] Hartland, J., Gregory-Smith, D., Harvey, N., and Rose, M., 2000, "Nonaxi-symmetric Turbine End Wall Design: Part II—Experimental Validation," ASME J. Turbomach., 122[2], pp. 286–293.

[5] Gregory-Smith, D., Ingram, G., Jayaraman, P., Harvey, N., and Rose, M., 2001, "Non-Axisymmetric Turbine End Wall Profiling," Proceedings of the Fourth European Conference on Turbo-Machinery.

[6] Brennan, G., Harvey, N., Rose, M., Fomison, N., and Taylor, M., 2003, "Improving the Efficiency of the Trent 500-HP Turbine Using Nonaxisymmetric End Walls—Part 1: Turbine Design," ASME J. Turbomach., 125[3], pp. 497–504.

[7] Rose, M., Harvey, N., Seaman, P., Newman, D., and McManus, D., 2001,"Improving the Efficiency of the Trent 500 HP Turbine Using Non-Axisymmetric End Walls. Part II: Experimental Validation," ASME Paper No.2001-GT-0505.

[8] Diego Torre, Elena de la Rosa Blanco, Raúl Vázquez, and Howard P. Hodson, "A New Alternative for Reduction of Secondary Flows in Low Pressure Turbines," ASME Paper No.2006GT-91002.

[9] Dieter E. Bohn, Norbert Sürken, Qing Yuand Franz Kreitmeier, "Axisymmetric Endwall Contouring in a Four-stage Turbine-comparison of Experimental and Numerical Results," ASME Paper No. GT-2002-30351.

[10] Alexander Hergt, Robert Meyer and Karl Engel, "Effects of Vortex Generator Application on the Performance of a Compressor Cascade," ASME Paper No. GT2010-22464.

[11] Steffen Reising, Heinz-Peter Schiffer, "Non-axisymmetric End Wall Profiling in Transonic Compressors. Part 1: Improving the Static Pressure Recovery at Off-design conditions by Sequential Hub and Shroud End Wall Profiling," ASME Paper No. GT2009-59133.

[12] Grant Ingram, David Gregory-Smith, Neil Harvey, "Investigation of a Novel Secondary Flow Feature in a Turbine Cascade With End Wall Profiling," ASME J. Turbomach., 127, pp. 209–214.

[13] Harvey N.W., Brennan G., Newman D. A., and Rose M. G., "Improving Turbine Efficiency Using Non-axisymmetric End Walls: Validation in the multi-row Environment and With Low Aspect Ratio Blading," ASME Paper No. GT-2002- 30337.

[14] Harvey, N., 2008, "Some Effects of Non-Axisymmetric End Wall Profiling on Axial Flow Compressor Aerodynamics-Part I: Linear Cascade Investigation," ASME Paper No. GT2008-50990.

[15] Voss, C., Aulich, M., Kaplan, B., and Nicke, E., 2006, "Automated Multiob- jective Optimization in Axial Compressor Blade Design," ASME Paper No. GT2006-90420.

[16] Dorfner, C., Nicke, E., and Voss, C., 2007, "Axis-Asymmetric Profiled End-wall Design Using Multi-objective Optimization Linked With 3D RANS-Flow-Simulation," ASME Paper No. GT2007-27268.